Available online at www.sciencedirect.com
SCIENCE DIRECT®
Journal of Solid State Chemistry 176 (2003) 180–191
JOURNAL OF SOLID STATE CHEMISTRY
http://elsevier.com/locate/jssc

Investigation of structural and dynamic properties of $NH_4[N(CN)_2]$ by means of X-ray and neutron powder diffraction as well as vibrational and solid-state NMR spectroscopy

Bettina V. Lotsch,[a] Jürgen Senker,[a] Winfried Kockelmann,[b] and Wolfgang Schnick[a,*]

[a] *Department Chemie, Ludwig-Maximilians-Universität München, Butenandtstraße 5–13(D), D-81377 München, Germany*
[b] *Mineralogisch-Petrologisches Institut Universität Bonn, Poppelsdorfer, Schloss, D-53115 Bonn, Germany & ISIS Facility, Rutherford Appleton Laboratory, Chilton, Didcot OX11 0QX, UK*

Received 18 April 2003; received in revised form 17 June 2003; accepted 3 July 2003

Abstract

The crystal structure, spectroscopic and thermal properties of ammonium dicyanamide $NH_4[N(CN)_2]$ have been thoroughly investigated by means of temperature-dependent single-crystal X-ray and neutron powder diffraction, vibrational and MAS-NMR spectroscopy as well as thermoanalytical measurements. The comprehensive elucidation of structural details is of special interest with respect to the unique solid-state transformation of ammonium dicyanamide into dicyandiamide. This reaction occurs at temperatures $>80°C$ and it represents the isolobal analogue of Wöhler's historic transformation of ammonium cyanate into urea. $NH_4[N(CN)_2]$ crystallizes in the monoclinic space group $P2_1/c$ with lattice constants $a = 3.7913(8)$, $b = 12.412(2)$, $c = 9.113(2)$ Å, $\beta = 91.49(2)°$ and $Z = 4$ (single-crystal X-ray data, $T = 200$ K). The temperature dependence of the lattice constants shows anisotropic behavior, however, no evidence for phase transitions in the investigated temperature range was observed. The hydrogen positions could be localized by neutron diffraction (10–370 K), and the temperature-dependent behavior of the ammonium group has been analyzed by Rietveld refinements using anisotropic thermal displacement parameters. They were interpreted by utilizing a rigid body model and extracting the libration and translation matrices of the ammonium ion by applying the TLS formalism. The results obtained by the diffraction methods were confirmed and supplemented by vibrational spectroscopy and solid-state ^{15}N and ^{13}C MAS-NMR investigations.

Keywords: Crystal structure; Dicyanamide; Neutron diffraction; NMR; Rigid body

1. Introduction

Over the last decade, considerable research efforts have been focused on the synthesis of two- and three-dimensional structures with C_3N_4 stoichiometry, owing to the predicted ultra-hardness combined with thermal stability of such lightweight materials [1–3]. Recently, the focus on carbon nitride chemistry has been foremost centered on potential molecular precursors for the synthesis of extended g-C_3N_4-like networks.

On this background, simple inorganic nitridocarbonates (**IV**) such as cyanamides and dicyanamides, containing the linear $[N=C=N]^{2-}$ and bent planar $[N(CN)_2]^-$ anions, respectively, have been investigated. Among these, the cyanamides and dicyanamides of the metals M = Li [4,5], Na [6,7], K [8,9], Cs [10], Ag [11–13], Mg, Ca, Sr, Ba [14–16], Zn [17–19], Pb [20] and Co, Ni, Cu [21–23] have been structurally characterized. A particularly intriguing feature of dicyanamide chemistry is the thermal behavior of the alkali salts Li–Rb: upon heating, the $[N(CN)_2]^-$ anions undergo trimerization forming the respective tricyanomelaminate salts $M_3[C_6N_9]$ [5,7,9]. In this context, the investigation of the ammonium salt of dicyanamide $NH_4[N(CN)_2]$ (**1**) is of special interest since it combines interesting structural features with a unique thermally induced solid-phase reactivity: at temperatures above 80°C, the solid–solid isomerization into dicyandiamide $H_4C_2N_4$ (**2**) is observed [24,25]. This reaction represents the isolobal analogue of Wöhler's historic synthesis of urea starting from ammonium cyanate (Fig. 1).

*Corresponding author. Fax: +49-89-2180-77440.
E-mail address: wolfgang.schnick@uni-muenchen.de (W. Schnick).

0022-4596/$ - see front matter © 2003 Elsevier Inc. All rights reserved.
doi:10.1016/S0022-4596(03)00388-8

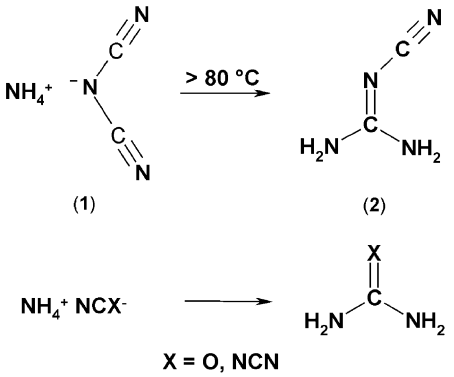

Fig. 1. Transformation of ammonium dicyanamide (**1**) into dicyandiamide (**2**) in the solid phase. The reaction represents the isolobal analogue to Wöhler's historic transformation of ammonium cyanate into urea.

The X-ray crystal structure of $NH_4[N(CN)_2]$ has been communicated recently [25]; however, no detailed information concerning the thermal behavior has been given yet. In this contribution we report on the synthesis and crystal structure characterization by both X-ray and neutron powder diffraction in a large temperature range between 10 and 370 K, as well as thermoanalytical and spectroscopic investigations. The transformation of $NH_4[N(CN)_2]$ into dicyandiamide $H_4C_2N_4$ and detailed studies on the temperature-dependent dynamics of the ND_4^+ group based on solid-state NMR spectroscopic investigations will be published in a forthcoming paper.

2. Experimental

2.1. Synthesis

$NH_4[N(CN)_2]$ was prepared by ion exchange in aqueous solution. A column containing an ion exchange resin in strongly acidic form (Merck, Ionenaustauscher I, H^+-Form, Art. 4765) was loaded with an aqueous solution of NH_4Cl (Fluka, $\geqslant$98%, 1–2.5 M) and thoroughly washed with deionized water to remove excess chloride. Subsequently, a solution containing $Na[N(CN)_2]$ (Fluka, $\geqslant$96%, 0.5 M) was poured onto the column. The eluate, evaporated at room temperature, gave a crop of colorless, needle-shaped crystals (yield $\approx$100%). For the neutron diffraction measurements, 3.0 g $NH_4[N(CN)_2]$ were dissolved in 20 mL D_2O (Deutero GmbH, 99.9%) and stirred under argon at 50°C. After 1 h, the D_2O was completely removed in vacuo. To yield the fully deuterated product, the former procedure was repeated twice and the white powdered product stored in a Schlenk flask under argon.

2.2. Vibrational spectroscopy

FTIR spectra of $NH_4[N(CN)_2]$ were recorded at room temperature on a Bruker IFS 66v/S spectrometer. The samples were thoroughly mixed with dried KBr and compressed to pellets (500 mg KBr/5 mg sample).

Raman spectra were recorded on a Spectrum 2000 NIR-FT-Raman spectrometer (Perkin–Elmer) which is equipped with a Nd–YAG laser optics system ($\lambda = 1064$ mm). During the measurements at room temperature, the sample (30 mg) was contained in a glass tube (diameter 2 mm) open to the atmosphere.

2.3. X-ray-diffraction

X-ray diffraction data of a single crystal were collected on a four-circle diffractometer (STOE Stadi 4) using graphite monochromated Mo*K*á radiation ($\lambda_{K\alpha} = 71.073$ pm). Complete data sets were recorded between 200 and 340 K using a 600 Series Cryostream Cooler (Oxford Cryosystems). The space group could be unambiguously determined as $P2_1/c$ (No. 14). The crystal structure was solved by direct methods using the software package SHELXS-97 [26] and refined using SHELXL-97 [27] with anisotropic displacement parameters for all non-hydrogen atoms.

Further details of the crystal structure determination reported in this paper may be obtained from the Fachinformationszentrum Karlsruhe, D-76344 Eggenstein-Leopoldshafen, Germany, by quoting the depository number CSD-413097.

Temperature-dependent in situ X-ray diffractometry was performed on an STOE Stadi P powder diffractometer (Cu$K\alpha_1$ radiation, $\lambda_{K\alpha_1} = 154.051$ pm), which is equipped with a 600 Series Cryostream Cooler (Oxford Cryosystems) for measurements below room temperature.

2.4. Neutron powder diffraction

Time-of-flight (TOF) neutron diffraction data of a deuterated sample of ammonium dicyanamide were obtained on the ROTAX instrument at the ISIS spallation source of the Rutherford Appleton Laboratory, UK [28]. The polycrystalline sample (deuteration grade >95% as determined by solid-state NMR and IR spectroscopy as well as mass spectrometry) was transferred into a vanadium vessel (length 60 mm, diameter 8 mm) in a glove-box and sealed air-tight using copper rings. Data were collected on two medium resolution banks in forward scattering geometry and a high-resolution backward scattering bank being composed of linear position-sensitive ^{6}Li glass scintillation detector systems. A prominent feature of the ROTAX-TOF

instrument is the constant high resolution $\Delta d/d = 0.0035$ (d is the lattice spacing) in backscattering geometry (for higher order reflections). The detector banks cover a TOF range from 2.4 to 12.0 ms ($d = 202-998$ pm), 2.7 to 20.0 ms ($d = 80-595$ pm) and from 4.0 to 19.4 ms ($d = 60-290$ pm) at diffraction angles $2\theta = 17.2°$, 52.6° and 122.0°, respectively. The data were normalized with respect to those of a standard vanadium sample. Complete powder diffraction patterns were recorded at temperatures between 10 and 370 K at 13 different temperatures using a hot-stage closed-cycle refrigerator [29] with a Eurotherm type 2408 temperature control (Eurotherm Controls Limited), the Pt sensor (Pt 100) being in contact with a copper block mounted on top of the vanadium can. For safety reasons, there was no heat exchange gas in the chamber surrounding the sample. A thin vanadium foil radiation shield was used as thermal shielding against ambient temperatures. Accordingly, the copper block served as the major heat transfer medium and thus, a heat gradient within the sample container occurred. The acquisition time for the low-temperature runs was typically 2 h, whereas the data sets at 10 K and room temperature were collected within 6 h.

The data of the three detector banks were refined simultaneously with the structure refinement program GSAS, which is based on the Rietveld method [30,31] (Fig. 2). Anisotropic atomic displacement parameters were used for the deuterium atoms and the ammonium-nitrogen from 10 to 365 K. The profile of the ROTAX-TOF data could satisfactorily be described by a convolution of two back-to-back exponentials with a pseudo-Voigt function, the background was modeled using a Chebyschev polynomial of the first kind with typically 12 coefficients [31]. The cell constants, atomic, line shape and background parameters were varied simultaneously, whereas the characteristic diffractometer constants were kept at their original values in order to obtain accurate lattice constants. For the investigation of the librational and translational dynamics of the ammonium group as a whole, the structural parameters of the ammonium group were parameterized as rigid body, using a model with four variable N–D bond lengths and a fixed tetrahedral angle (average D–N–D angle of the respective unrestrained refinement).

Further details of the neutron diffraction data recorded at 10 K may be obtained from the Fachinformationszentrum Karlsruhe, D-76344 Eggenstein-Leopoldshafen, Germany, by quoting the depository number CSD-413096.

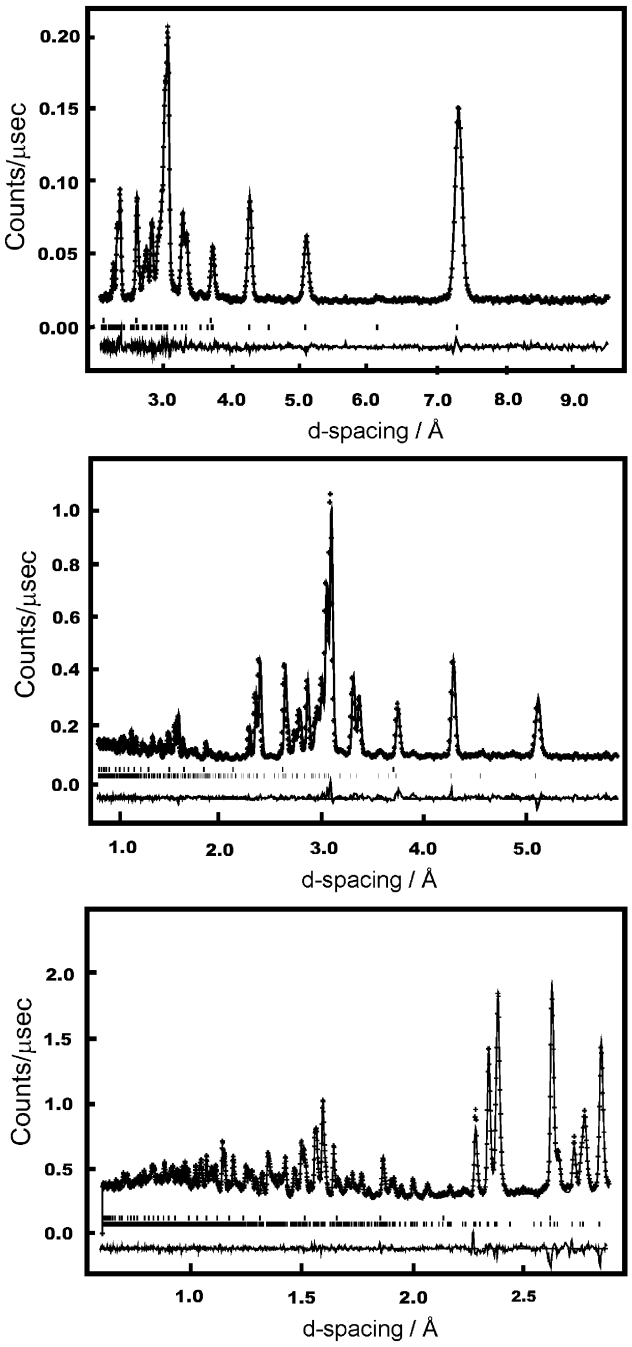

Fig. 2. Rietveld profile fits of $ND_4[N(CN)_2]$ at 10 K. Observed (crosses) and calculated (line) neutron powder diffractograms as well as difference profiles (lower line). The lower rows of vertical lines indicate the possible reflection positions of $ND_4[N(CN)_2]$ (lower row) and ND_4Cl (upper row). Top: bank 1 (2.4–12.0 ms, $d = 202-998$ pm, $2\theta = 17.2°$); middle: bank 2 (2.7–20.0 ms, $d = 80-595$ pm, $2\theta = 52.6°$), bottom: bank 3 (4.0–19.4 ms, $d = 60-290$ pm, $2\theta = 122.0°$).

2.5. Thermal analysis

Thermoanalytical measurements between room temperature and 300°C or 500°C were carried out using a Mettler DSC 25 (variable heating rates between 0.5°C/min and 50°C/min); for combined DTA/TG measurements in the same temperature range a Setaram thermoanalyzer TGA 92-2400 was used.

2.6. Solid-state NMR spectroscopy

^{13}C and ^{15}N CP-MAS-NMR studies have been conducted on a DSX Avance 500 solid-state NMR spectrometer (Bruker, Karlsruhe) equipped with two phase sensitive detectors in quadrature. The proton decoupled measurements using a commercial double-resonance MAS probe (Bruker, Karlsruhe) were carried out by transferring the powdered sample into a ZrO_2 rotor (diameter 4 mm) which was sealed by a pierced *h*-BN cap for pressure equalization. The MAS spectra were recorded with an eightfold phase cycled cross polarization (CP) impulse sequence (contact times 10 (^{13}C) and 20 ms (^{15}N)) at 5 (^{13}C) and 1.5 kHz (^{15}N) spinning frequency, respectively. The spinning frequencies were optimized in order to extract isotropic and anisotropic properties of the chemical shift interaction. The proton decoupling was effected by a two pulse phase modulation (TPPM) pulse sequence [32]. The spectra were simulated and iteratively fitted with the NMR simulation software package Simpson [33].

Table 1
X-ray crystallographic data for $NH_4[N(CN)_2]$

Formula	$NH_4[N(CN)_2]$
Diffractometer, monochromator	STOE STADI 4, graphite
Radiation	Mo$K\alpha$ ($\lambda = 71.073$ pm)
Temperature (K)	200
Space group	$P2_1/c$ (No. 14)
Lattice constants (Å, °)	$a = 3.7913(8)$
	$b = 12.412(2)$
	$c = 9.113(2)$
	$\beta = 91.49(2)$
Cell volume (10^6 pm^3)	$V = 428.66(12)$
Formula units	$Z = 4$
Calc. density (g cm^{-3})	1.303
Diffraction range (°)	$5.5 < 2\theta < 55$
Scan type	ω
Observed reflections	1923
Independent reflections	979 ($R_{int} = 0.034$)
$F(000)$	176
Corrections	Lorentz, polarisation, extinction
Extinction coefficient	$\chi = 0.048(11)$
Refined parameters	72
R indices (for all data with $F_o^2 \geqslant 2\sigma F_o^2$)	$R_1 = 0.0357$
	w$R_2 = 0.1000$
	$w^{-1} = \sigma^2 F_o^2 + 0.0475P^2 + 0.0497P$
GooF	1.091
Min./max. residual electron density ($e^- \times 10^{-6}$ pm^{-3})	−0.174/0.160

3. Results and discussion

3.1. Crystal structure

Details of the X-ray crystal structure solution and refinement are summarized in Table 1, lists of the positional coordinates and displacement parameters are given in Table 2. $NH_4[N(CN)_2]$ is built up from crystallographically equivalent NH_4^+ and $[N(CN)_2]^-$ ions, respectively, which are alternately stacked forming parallel chains along [001] (Fig. 3). The monoclinic unit cell contains four formula units of which one is

Table 2
Positional coordinates and displacement factors (in pm^2, standard deviations in brackets) of $NH_4[N(CN)_2]$ (X-ray single-crystal data at 200 K, upper row) and $ND_4[N(CN)_2]$ (neutron powder diffraction data at 10 K, obtained from Rietveld refinements, lower row)

Atom	x	y	z	U_{eq}/U_{iso}	U_{11}	U_{22}	U_{33}	U_{23}	U_{13}	U_{12}
N1	0.5605(3)	0.38261(9)	−0.1159(2)	0.0366(3)	0.0470(7)	0.0405(6)	0.0225(5)	−0.0015(4)	0.0044(4)	−0.0021(5)
	0.5476(7)	0.3837(2)	−0.1151(3)	0.0131(6)						
C1	0.4917(3)	0.35899(9)	0.0021(2)	0.0271(3)	0.0335(6)	0.0248(5)	0.0229(5)	−0.0025(4)	−0.0020(4)	−0.0017(4)
	0.4816(9)	0.3604(3)	0.0027(4)	0.011(9)						
N2	0.3914(3)	0.32232(9)	0.1302(2)	0.0369(3)	0.0557(7)	0.0354(6)	0.0195(5)	−0.0009(4)	−0.0006(4)	−0.0188(5)
	0.3811(7)	0.3235(2)	0.1298(4)	0.0133(6)						
C2	0.4894(3)	0.37123(8)	0.2516(2)	0.0256(3)	0.0302(6)	0.0236(5)	0.0231(5)	0.0036(4)	0.0009(4)	−0.0031(4)
	0.4812(9)	0.3705(4)	0.2511(4)	0.0124(8)						
N3	0.5569(3)	0.40782(8)	0.3656(2)	0.0322(3)	0.0441(6)	0.0308(5)	0.0214(5)	−0.0006(4)	−0.0030(4)	−0.0038(4)
	0.5501(7)	0.4081(2)	0.3661(3)	0.0101(6)						
N4	0.0041(3)	0.11548(8)	0.1341(2)	0.0257(3)	0.0293(5)	0.0264(5)	0.0212(5)	−0.0016(4)	−0.0012(4)	−0.0009(4)
	−0.0010(7)	0.1124(2)	0.1324(4)	0.0140	0.015(2)	0.009(1)	0.018(1)	−0.002(2)	−0.001(1)	−0.003(1)
H1	0.151(4)	0.059(2)	0.139(2)	0.042(4)						
D1	0.175(1)	0.0500(4)	0.1349(5)	0.0296	0.023(3)	0.044(3)	0.022(3)	0.005(2)	0.003(2)	0.019(2)
H2	−0.126(4)	0.112(2)	0.052(2)	0.037(4)						
D2	−0.162(1)	0.1084(4)	0.0391(5)	0.0206	0.028(3)	0.019(2)	0.014(2)	−0.000(2)	−0.005(2)	−0.001(2)
H3	−0.124(5)	0.114(2)	0.216(2)	0.042(4)						
D3	−0.158(1)	0.1104(5)	0.2258(4)	0.0287	0.035(3)	0.032(3)	0.019(2)	−0.003(3)	0.008(2)	−0.002(3)
H4	0.125(4)	0.177(2)	0.132(2)	0.039(4)						
D4	0.141(1)	0.1832(3)	0.1356(6)	0.0300	0.041(3)	0.013(2)	0.036(3)	0.001(2)	−0.004(3)	−0.005(2)

All atoms on Wyckoff position 4e, SOF = 1. U_{eq} is defined as one-third of the trace of the orthogonalized U_{ij} tensor.

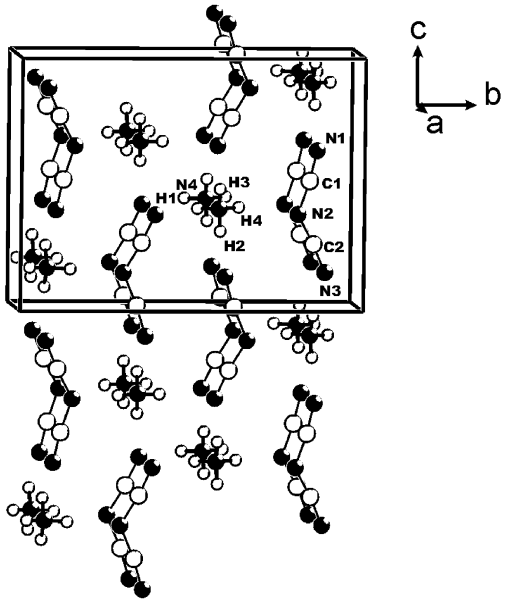

Fig. 3. Crystal structure of $NH_4[N(CN)_2]$, view along [100]. N: black circles, C: big white circles, H: small white circles.

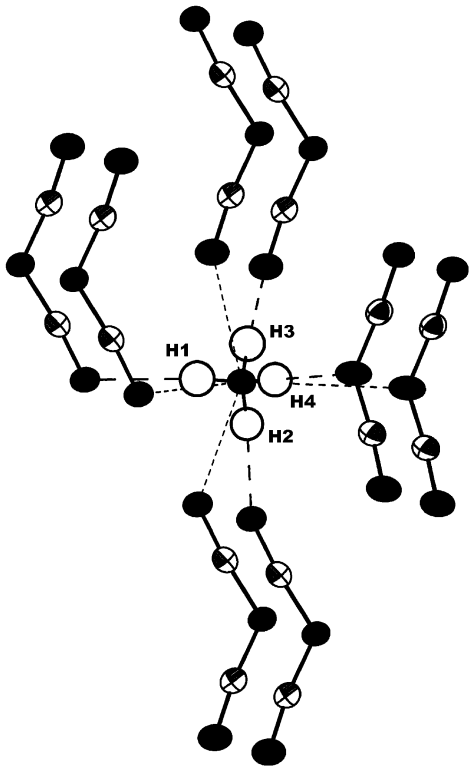

Fig. 4. Coordination sphere of the ammonium ions in $NH_4[N(CN)_2]$, displacement ellipsoids are drawn at the 50% probability level. N: black ellipsoids, C: white ellipsoids, H: white circles.

symmetrically independent. The coordination sphere of the ammonium ion can be described as that of a distorted cube, the corners being composed of eight dicyanamide ions. Six of these are terminal N and two are bridging amido N of the dicyanamide ions, resulting in four short N4···N contacts (287–307 pm) and four longer contacts ranging from 307 to 346 pm (Fig. 4). Relevant bond distances and angles can be found in Table 3.

The bent planar dicyanamide ions exhibit only minor deviations from point symmetry C_{2v}, the bond distances and angles being similar to those of other ionic dicyanamides. The bond lengths correspond to the formula $[N{\equiv}C{-}N{-}C{\equiv}N]^-$ with localized single (131 pm) and triple bonds (115–116 pm). The data sets recorded at higher temperatures (250–340 K) confirm the structure model of the low-temperature data. No significant change of the structural parameters other than the expected increase of the temperature factors and anisotropic thermal expansion was detected (see below), the *R*-factors being similar to those of the low-temperature data (wR_2: 10.0–11.0%, R_1: 3.6–3.7%, R_{int}: 3.4–2.2%, goodness-of-fit (Goof): 1.091–1.063, 200 → 340 K).

Besides the completion of the structural model obtained from single-crystal X-ray investigations, the accurate position of the hydrogen atoms is of special interest with respect to the temperature-dependent dynamics of the NH_4^+ group and reactivity of ammonium dicyanamide. For this purpose, neutron diffraction data were collected at 10 K for a fully deuterated sample of ammonium dicyanamide. Details of the neutron diffraction experiment and Rietveld refinement at 10 K are listed in Table 4, the atomic coordinates and displacement parameters are given in Table 2. The structure model obtained from the Rietveld refinement is consistent with the single-crystal X-ray investigations at 200 K. The positions of the hydrogen atoms could be unambiguously established from the simultaneous Rietveld refinement of the three detector banks (for further details see below), the four D···N hydrogen bridge contacts range from 185 to 203 pm.

The hydrogen bridge network is believed to play a major role in terms of a pre-orientation of the ionic reactants towards each other, and thus to influence the high-temperature reactivity of the compound. A prominent feature of the medium strong hydrogen bridge ensemble is the partition into two weaker (i.e. longer, N4–D1···N3/N4–D4···N2) and two stronger (i.e. shorter, N4–D2···N3/N4–D3···N1) hydrogen bridges, the latter being roughly directed along the crystallographic *c*-axis, while the former run perpendicular to it. These findings may be indicative of the fixation of the ammonium ion by the two stronger hydrogen bridges which may significantly direct the dynamics of the ammonium group as a whole and affect the trajectories of the deuterium atoms in particular.

Table 3
Intra- and intermolecular bond distances (in pm) and angles (in °) for $NH_4[N(CN)_2]$ (200 K, 2. and 5. column) and $ND_4[N(CN)_2]$ (10 K, 3. and 6. column)

N4–H1	90(2)	101.1(4)	H1–N4–H2	110(1)	110.2(5)
N4–H2	89(2)	103.0(5)	H1–N4–H3	107(1)	110.0(5)
N4–H3	90(2)	104.9(5)	H1–N4–H4	111(2)	108.2(4)
N4–H4	90(2)	102.0(5)	H2–N4–H3	114(1)	110.2(4)
C1–N1	115.1(2)	114.6(4)	H2–N4–H4	107(1)	110.8(5)
C2–N3	115.7(2)	117.0(4)	H3–N4–H4	108(1)	107.4(5)
N2–C1	131.8(2)	131.1(4)	C1–N2–C2	120.5(1)	121.3(4)
N2–C2	130.7(2)	129.4(4)	N1–C1–N2	173.2(1)	172.5(4)
			N3–C2–N2	173.7(1)	174.5(5)
N4⋯ N1	287(3)	289.4(4)	N4–H1–N3	172(2)	169.8(4)
	307(3)	304.1(4)			
N4⋯N2	295.8(2)	296.7(4)	N4–H2–N3	175(2)	176.5(4)
	346.2(2)	347.6(5)			
N4(−H1)⋯N3	306.8(2)	302.7(4)	N4–H3–N1	175(2)	175.7(5)
	334.2(2)	324.6(4)			
N4(−H2)⋯N3	295(3)	292.5(4)	N4–H4–N2	178(2)	175.0(4)
	328(3)	323.8(5)			

Table 4
Neutron diffraction and Rietveld refinement data for $ND_4[N(CN)_2]$

Diffractometer	ROTAX, ISIS
Temperature (K)	10
Lattice parameters (Å, °)	$a = 3.7328(1)$
	$b = 12.3177(3)$
	$c = 9.1303(3)$
	$\beta = 91.596(2)$
Cell volume (10^6 pm^3)	$V = 419.64(2)$
Calc. density (g cm^{-3})	1.395
Scan mode	TOF
2θ (banks 1–3)	17.24, 52.62, 122.18
Range of d-spacings (Å) (banks 1–3)	2.0–10.0, 0.8–5.9, 0.7–2.9
Number of Bragg reflections (all banks)	3370
Absorption coefficient (cm^{-1})	$\mu = 0.1448$
Refined parameters	87
R values (banks 1–3)	R_{wp}: 0.0403, 0.0337, 0.0438
	R_{F^2}: 0.0318, 0.0302, 0.0217
	R_{Bsq}: 0.0200, 0.0302, 0.0247
Red. χ^2	1.950

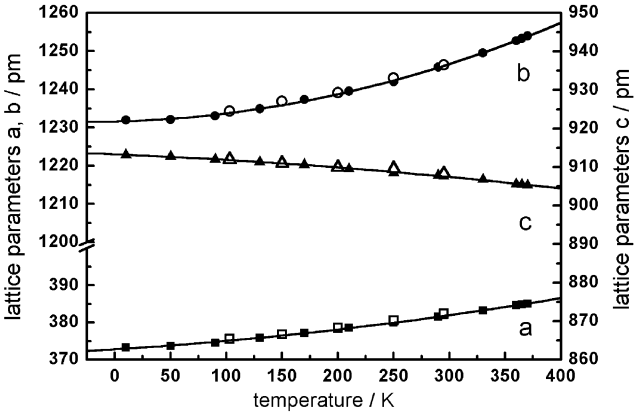

Fig. 5. Thermal behavior of the lattice constants of $NH_4[N(CN)_2]$ and $ND_4[N(CN)_2]$ as monitored by temperature-dependent X-ray powder diffraction between 100 and 298 K (open symbols) and neutron powder diffraction between 10 and 370 K (filled symbols), respectively. Both neutron and X-ray data are interpolated by second-order polynomials (solid lines).

3.2. Thermal behavior of the lattice and atomic parameters

The lattice parameters and cell volume of ammonium dicyanamide were determined by both X-ray and neutron diffraction at various temperatures. The results are shown in Figs. 5 and 6. Both diffraction methods reveal the same tendencies, of which the most striking one is the pronounced anisotropic thermal expansion of the lattice parameters in the temperature range investigated (a: +1.8%, b: +1.0%, c: −0.4%, β: +0.1%). Whereas the a- and b-axis show normal thermal expansion with increasing temperature, the c-axis exhibits a negative coefficient of thermal expansion. The thermal behavior of the cell volume, which is relevant for the evaluation of possible phase transitions, is shown in Fig. 6. Both X-ray and neutron diffraction data indicate a normal thermal expansion without any evidence of structural phase transitions in this temperature range. The systematically lower values obtained from neutron diffraction may be due to the insufficient temperature transfer and the resulting heat gradient within the sample tank.

Besides the temperature dependence of the lattice constants, the thermal behavior of the anisotropic displacement amplitudes and certain geometric parameters of the ammonium group have been investigated on the basis of unrestricted anisotropic refinements of the data sets between 10 and 370 K. Importance was primarily attached to thermal changes with respect to the deuterons, insofar as the latter serve as main indicators for underlying changes of the dynamics and

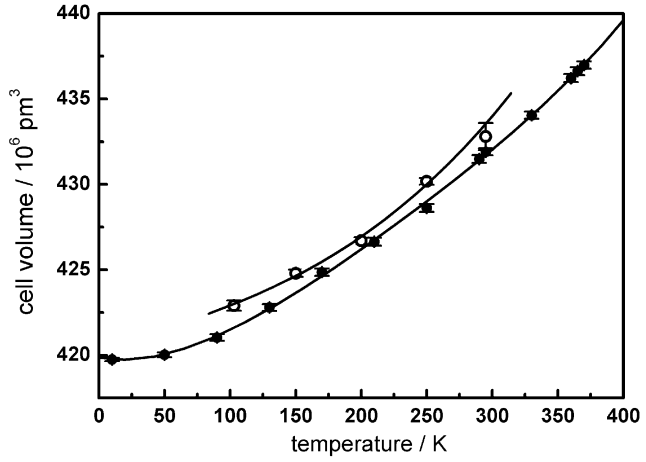

Fig. 6. Thermal behavior of the cell volume of ammonium dicyanamide as monitored by temperature-dependent X-ray (open symbols) and neutron powder diffraction (filled symbols) from 100 to 298 K and 10 to 370 K, respectively. Both data sets are interpolated by fourth-order polynomials (solid lines).

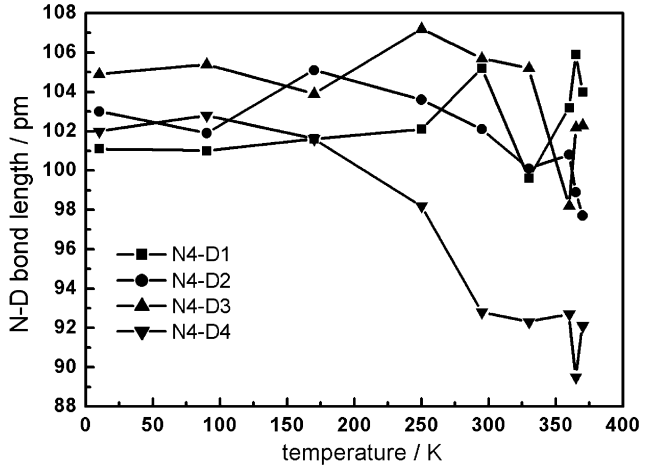

Fig. 7. Thermal behavior of the N–D bond lengths without libration correction, based on the anisotropic Rietveld refinements of the neutron diffractograms recorded between 10 and 370 K.

reactivity of the ammonium group. According to the enhanced thermal movement of the deuterons, the anisotropic displacement factors steadily increase with temperature. Whereas the temperature factors of the deuterons D2–D4 increase about linearly, those of D1 can be approximated by a parabolic interpolation, indicating a more pronounced thermal movement of the latter deuteron. The N4–D bond lengths (Fig. 7) similarly show a rather heterogeneous behavior in that the N4–D4 distance severely drops at high temperatures, whereas the other bond lengths remain practically constant taking into account the error of experimental data. This result might be tentatively correlated with the nature of the hydrogen bond network. The latter does not exhibit unexpected changes with temperature. The contacts D2⋯N3 and D3⋯N1 range between 185 and 199 pm while D1⋯N3 and D4⋯N2 amount to 195–217 pm within the temperature interval of 360 K, again reflecting the pertaining partition into two stronger and two weaker contacts. The angles N4–D⋯N associated with the hydrogen bridges do not alter considerably with temperature either; however, the angles involving the deuterons D1 and D4 (170°→164°, 175°→165°) generally deviate from 180° more significantly than those involving D2 and D3 (176°→175°, 176°→177°), which is also consistent with the differentiation into two weaker and two stronger hydrogen bonds. The D–N–D tetrahedral angles remain largely undistorted until room temperature, while above 300 K the angles D2–N4–D4 and D3–N4–D4 significantly widen (→120°, →117°), whereas D1–N4–D4 decreases considerably (→99°).

3.3. Librational and translational motion of the ND_4^+ group

In order to yield information about the low-temperature motional behavior of the ammonium ion, a parameterization of the anisotropic displacement parameters was carried out. The separation of the librational, translational (external modes) and vibrational modes (internal modes) is based on the implementation of a rigid body model, which, however, has physical significance only if the amplitudes of the internal modes are negligible compared to those of the external modes. This can be assumed to be applicable in this case as is for most of the N–D bonds [34,35]. The mean-square displacements of the ammonium ion can be described in terms of a (symmetric) translation matrix **T**, a (symmetric) libration matrix **L**, and a (non-symmetric) correlation matrix **S** [36], taking into account the existence of mixed translational–librational modes. The center of gravity (N4) of the cation was chosen to be the molecular center for the parameterization and thus coincides with the origin of the Cartesian reference coordinate system in which the TLS matrices are defined. Since the monoclinic angle is very near to 90° (91.3° at 10 K), the reference coordinate system is almost aligned with the crystallographic coordinate system. In this case, where the molecular center is identical with the center of gravity location, the correlation matrix can be set to zero as is stated in the literature [37]. Since all ammonium ions are located on general positions, no geometric restrictions of the **L** and **T** matrices must be considered a priori. Some of the most relevant refinement parameters of the rigid body fit at 10 K are listed in Table 5. The *R*-values of the rigid body refinements did not significantly deteriorate compared to the unrestricted refinements.

From the eigenvalues and the direction cosines belonging to the eigenvectors of the diagonalized

Table 5
Refined parameters of the rigid body fit, based on the neutron diffraction data for $ND_4[N(CN)_2]$ at 10 K. Top lines: orientation and positional parameters R_i (°) and T_i (Å) for transferring the internal rigid body coordinate system into the crystal coordinate system. Middle and bottom rows: elements of the translation and libration tensors **T** (Å^2) and **L** ((°)^2)

$R_z(\alpha_z)$	$R_y(\alpha_y)$	$R_x(\alpha_x)$	T_x	T_y	T_z
−158(6)	88.4(1)	64(6)	−0.0004(4)	0.1133(1)	0.1334(2)
T_{11}	T_{22}	T_{33}	T_{12}	T_{13}	T_{23}
0.014(1)	0.0121(8)	0.0163(9)	−0.0033(9)	0.0007(6)	0.000(1)
L_{11}	L_{22}	L_{33}	L_{12}	L_{13}	L_{23}
43(7)	68(5)	91(5)	−4(5)	20(4)	−7(9)

libration matrix one can derive an axis, termed L_{33}, which is associated with the direction perpendicular to the major librational degrees of freedom. At low temperatures, L_{33} encloses only a small angle with the crystallographic *c*-axis so that the largest amplitudes of libration may be associated with the N4–D1 and N4–D4 bonds since they are aligned almost perpendicular to the *c*-axis. This, however, is in agreement with the findings that the bonds N4–D2 and N4–D3 are more strongly involved in the hydrogen bridge network and therefore less spatially mobile. Whereas at low temperatures, the direction of the major libration axis can be roughly associated with the bond N4–D2, the axis continuously inclines towards the plane perpendicular to the *c*-axis (001) (quadrant enclosed by the positive *a*- and *b*-axis) at higher temperatures and approaches the direction of the N4–D4 bond (Fig. 8). The maximum librational root-mean-square amplitudes L_{33} range from 10° at 10 K to 17° at 365 K.

As for the librational mobility of the ammonium ion, its translation is clearly anisotropic in nature. The maximum root-mean-square translational displacements can be associated with a major axis of translation, termed T_{33}, whereas in the perpendicular directions, the translational amplitudes T_{11} and T_{22} are persistently smaller. The principal axis system of the translation tensor coincides with the principal axis system of the anisotropic displacement of the central nitrogen atom. The root-mean-square displacements of the diagonalized translation tensor amount to 10–13 pm at 10 K and 16–24 pm at 365 K.

To illustrate the spatial distribution of the nuclear density as is contained in the thermal displacement parameters, two-dimensional Fourier cuts of the ammonium group at various temperatures are shown in Fig. 9. The spatial distribution of the deuterium atoms is almost spherical at 10 K and no pronounced smearing of the deuterium density is detectable. As expected, this is indicative of a nearly static ammonium group exhibiting only small-angle librations of the deuterium atoms at this temperature. At higher temperatures, the probability density function (pdf) of the deuterium atoms D1 and D4 (left) is becoming increasingly anisotropic, which applies to the atoms D2 and D3 (right) to a much lesser extent. This nicely demonstrates the larger librational amplitudes associated with the deuterons D1 and D4 compared to D2 and D3. At temperatures higher than 330 K, the pdf of the central nitrogen becomes ellipsoidally distorted, reflecting the translational trajectory of the nitrogen N4 directed towards the N4–D1 bond.

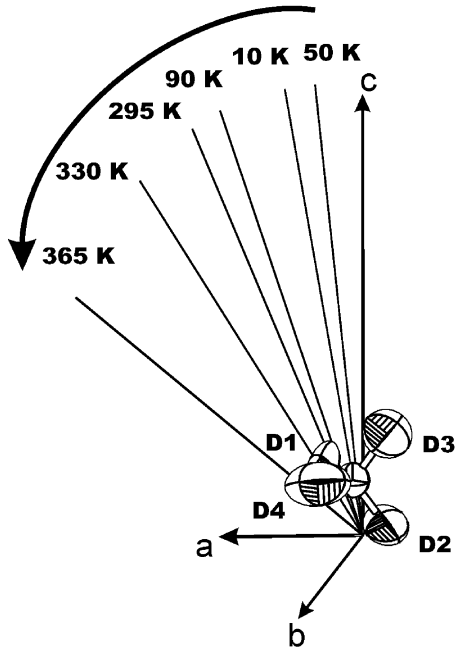

Fig. 8. Projection of the major axis of libration L_{33} into the origin of the unit cell at temperatures between 10 and 365 K. With increasing temperature, the inclination of the main libration axis towards the plane (001) is observable.

In order to obtain accurate bond length data taking into account the librational motion of the ammonium group, a libration correction based on the libration matrix **L** has been applied to the N–D bond lengths using the following equation:

$$\delta\vec{r}_k = -\tfrac{1}{2}[(Tr(\mathbf{L})\vec{r}_k - \mathbf{L}\vec{r}_k)]. \quad (1)$$

The corrected values together with the original ones are given in Table 6. The mean N–D bond lengths

averaged over the whole temperature range and over all four N–D bonds is 104 pm which is in good coincidence with the literature data [38–40]. Compared to the uncorrected values, the shortening due to libration is apparently compensated and variations with temperature are reduced. However, especially for N4–D4, bond distances $\leqslant 100$ pm do still occur at higher temperatures, which may be explained by inferring a weakening of the hydrogen bridges or complex dynamics of the ammonium group.

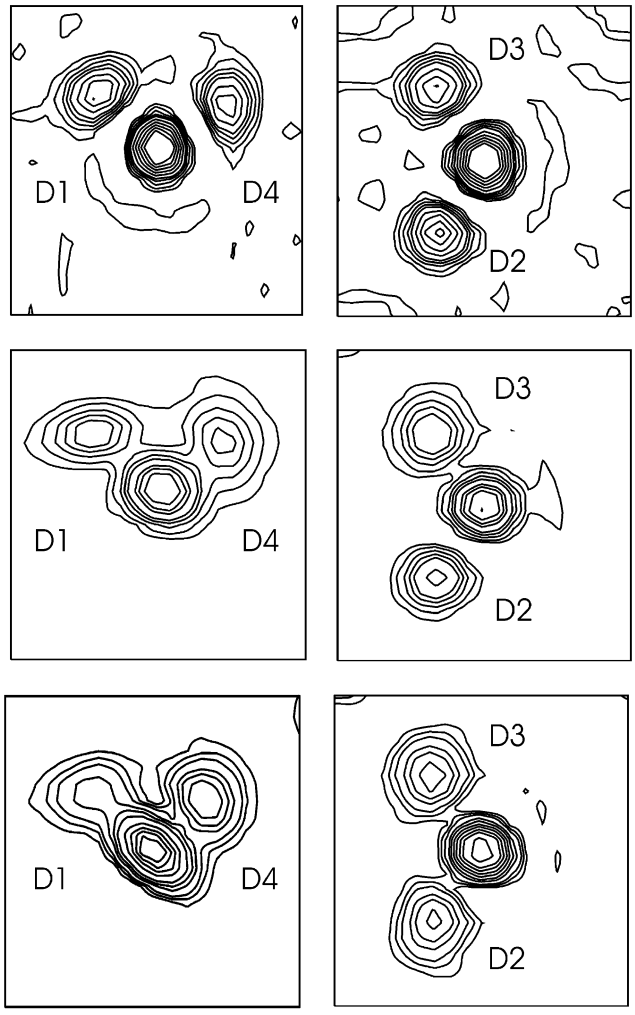

Fig. 9. Fourier cuts through the nuclear density of the ammonium group at temperatures 10, 295 and 365 K (top to bottom). Left: view onto the *ab*-plane (D1–N4–D4, map size 360×360 pm); right: view onto the *ac*-plane (D3–N4–D2, top to bottom, map size 360×360 pm). The center of reference is positioned at the (temperature-dependent) atomic coordinates of the ammonium nitrogen.

The results of the temperature-dependent neutron diffraction data are of special relevance for further dynamic investigations, since they can be interpreted in terms of the slowly proceeding onset of the solid–solid transformation of $NH_4[N(CN)_2]$ into $H_4C_2N_4$. The pre-orientation of the cations and anions as well as the hydrogen bridge contacts within the crystal are believed to be requisite for an initial proton transfer from the ammonium to the dicyanamide ion.

The contraction of the *c*-axis with increasing temperature can tentatively be correlated with the nature of the hydrogen bridge network which may be partitioned into two weaker hydrogen bridges (D1⋯N3, D4⋯N2) and two stronger ones (D2⋯N3 and D3⋯N1), the latter being oriented approximately along the direction of the *c*-axis. At higher temperatures it becomes evident that the librational and translational degrees of freedom are predominantly associated with the N4–D1 and N4–D4 bonds. On the one hand, this can be seen from the pronounced shortening of the N4–D4 bond which is presumably due to enhanced librational movement. On the other hand, a significant increase of the thermal displacement factor of D1 becomes evident at higher temperatures, which together with the translationally elongated pdf of N4 reflects thermally activated anisotropic movement along the N4–D1 bond direction.

It might therefore be concluded that an enhanced mobility of D1 is indicative of the commencing detachment of this deuteron which is subsequently transferred to the anion $[N(CN)]_2^-$. To clarify this issue as well as the exact proton transfer mechanism during the course of the isomerization, more detailed neutron diffraction and solid-state NMR studies are underway.

3.4. Vibrational spectroscopy

IR spectroscopic data of $NH_4[N(CN)_2]$ have already been communicated; however, assignments have only

Table 6
Uncorrected (left) and libration corrected (right) N–D bond lengths in $ND_4[N(CN)_2]$

T	N4–D1		N4–D2		N4–D3		N4–D4	
10	102.8(4)	105.0	104.7(4)	106.4	104.3(4)	106.6	102.4(4)	104.7
50	103.9(6)	106.3	105.3(6)	107.1	103.9(6)	105.9	101.7(6)	104.2
90	102.1(6)	104.5	105.5(6)	107.2	104.3(6)	106.4	102.4(6)	104.5
295	100.4(8)	103.6	102.3(7)	103.8	102.5(7)	104.4	94.7(9)	97.0
330	96.0(7)	99.4	103.1(7)	105.2	103.8(6)	106.8	95.6(9)	98.3
365	98.7(9)	104.8	100.2(9)	103.7	100.9(8)	105.7	94(1)	96.7

been made with respect to the dicyanamide ion [41,42]. In order to account for effects of the crystal symmetry on the vibrational spectrum of $NH_4[N(CN)_2]$, a factor group analysis based on the correlation method has been carried out [43]. Representative IR and Raman spectra of $NH_4[N(CN)_2]$ are shown in Fig. 10, the observed vibration bands together with their assignments are given in Table 7 [41–49]. The factor group analysis yields a total of 72 vibrational (internal) and 24 translational as well as 24 librational (external) modes due to the site symmetry 1 of all molecular ions and the unit cell content of $Z = 4$. The external modes, of which six acoustic translational modes have to be subtracted, are partially located in the low-frequency region at wavenumbers smaller than 400 cm^{-1} which is characterized by significant band overlap. The fact that hardly any splittings of the vibrational bands attributable to the free molecules are observed in the vibrational spectra of $NH_4[N(CN)_2]$ is indicative of only weak ionic interactions between the isolated molecular ions and hence negligible coupling of their vibrational modes.

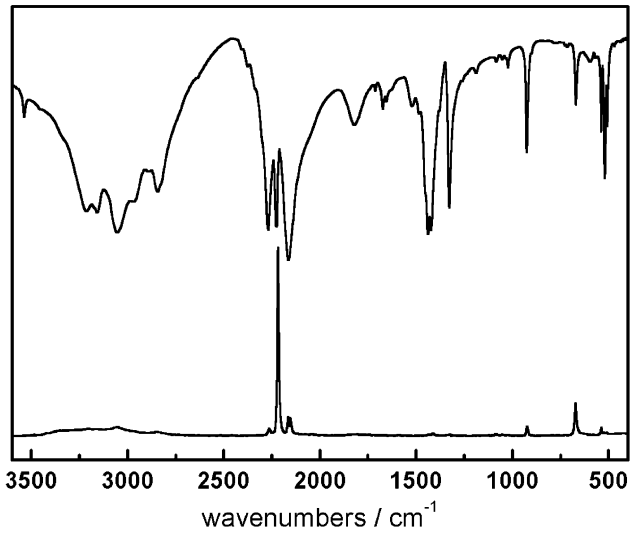

Fig. 10. FTIR (top) and FT-Raman spectrum (bottom) of $NH_4[N(CN)_2]$, both recorded at room temperature.

Table 7
Observed vibrational frequencies (in cm^{-1}) of $NH_4[N(CN)_2]$. The assignments with respect to the anion were made on the basis of the vibrational spectra of $N(CO)_2^+$ and N_5^+ [44,45], those of the cation with reference to solid ammonium chloride [48].

ν_{lit} [41,46,47]	ν_{obs} (IR)	ν_{obs} (Raman)	Assignment [44,45,48,49]
3538	3537		$\nu_s C{\equiv}N + \nu_{as} N{-}C$
3209	3214		$\nu_1 N{-}H + \nu_5 N{-}H$
3138	3158		ν_3 ($=\nu_{as}$) (F 2)
3044	3054	3050	$\nu_2 N{-}H + \nu_4 N{-}H$
3041	2967		ν_1 ($=\nu_s$) (A1)
2810	2843	2848	2 $\nu_4 N{-}H$
2274	2269	2267	$\nu_{as} N{-}C + \nu_s N{-}C$
2229	2225	2200	$\nu_s C{\equiv}N$ (A 1)
2171	2165	2169	$\nu_{as} C{\equiv}N$ (B 2)
1762	1821	1837	$\nu_4 N{-}H + \nu_6 N{-}H$
1710			$\nu_2 N{-}H$ ($=\delta_s$) (E)
1445	1438	1413	$\nu_4 N{-}H$ ($=\delta_{as}$) (F 2)
1328	1327	1325	$\nu_{as} N{-}C$ (B 2)
927	925	924	$\nu_s N{-}C$ (A 1)
668	670	671	$\delta_s C{-}N{-}C$ (A 1)
538	538	537	$\gamma_s N{-}C{\equiv}N$ (A 2)
519	519		$\gamma_{as} N{-}C{\equiv}N$ (B 1)
505	506		$\delta_{as} N{-}C{\equiv}N$ (B 2)
			$\delta_s N{-}C{\equiv}N$ (A 1)
359 (calc.)			$\nu_6 N{-}H$ (F 1)
168		176	$\nu_5 N{-}H$ (F 2)

3.5. Thermal analysis

Both calorimetric and thermogravimetric analyses exhibit an irreversible, strongly exothermic signal between 110°C and 150°C, depending on the heating rate and a less exothermic signal around 200°C. A DSC curve at a heating rate of 0.5°C/min is shown in Fig. 11. The first signal is attributable to the phase transition of $NH_4[N(CN)_2]$ to the isomeric dicyandiamide, whereas the second is assigned to the transformation of dicyandiamide into melamine. No phase transitions have been observed between room temperature and 100°C. The isomerization into dicyandiamide is accompanied by a weight loss of about 10%, being attributable to the thermal degasification of ammonia which is particularly pronounced in open systems. The enthalpy of transformation decreases continuously with increasing heating rate from roughly 56 to 13 kJ/mol which is most likely due to the increased tendency towards polymerization at higher heating ramps.

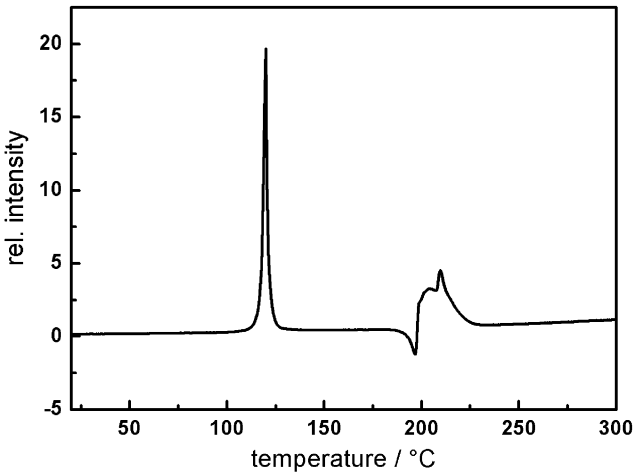

Fig. 11. DSC curve for $NH_4[N(CN)_2]$ between room temperature and 300°C, recorded at a heating rate of 0.5°C/min. Positive intensity values refer to exothermic caloric effects.

3.6. ^{13}C and ^{15}N CP-MAS-NMR studies

The crystallographic information obtained by powder and single-crystal methods is in good coincidence with the results of ^{13}C and ^{15}N CP-MAS-NMR studies of $NH_4[N(CN)_2]$ (Fig. 12). The ^{13}C spectrum exhibits two resonances assignable to the two different carbon atoms present in the dicyanamide molecule, whereas the ^{15}N spectrum shows the signals of the four nitrogen atoms distinguishable in cation and anion. These results coincide with the molecular ions being located on general sites within the unit cell which are all symmetrically equivalent.

The two nitrogen atoms of the nitrile group are shifted downfield with respect to the bridging and the ammonium nitrogen (σ_{iso} N1/N3: −216.8, −223.2 ppm, N2: −363.1 ppm, N4: −353.8 ppm) and exhibit the largest chemical shift anisotropy (σ_{aniso} N1/N3: −10024, −9668 Hz, N2: −3034 Hz). These findings may indicate rather static nitrile groups, whereas the chemical shift anisotropy of the ammonium nitrogen is strongly diminished by the local isotropy due to its approximate T_d geometry. Furthermore, the long ^{15}N CP contact time (20 ms) which was required to allow for an optimal polarization transfer is indicative of a high degree of rotational disorder of the ammonium ions at room temperature. The chemical shift anisotropy for N4 can therefore not be determined unambiguously from the simulated data (δ_{aniso} N4: 200–400 Hz).

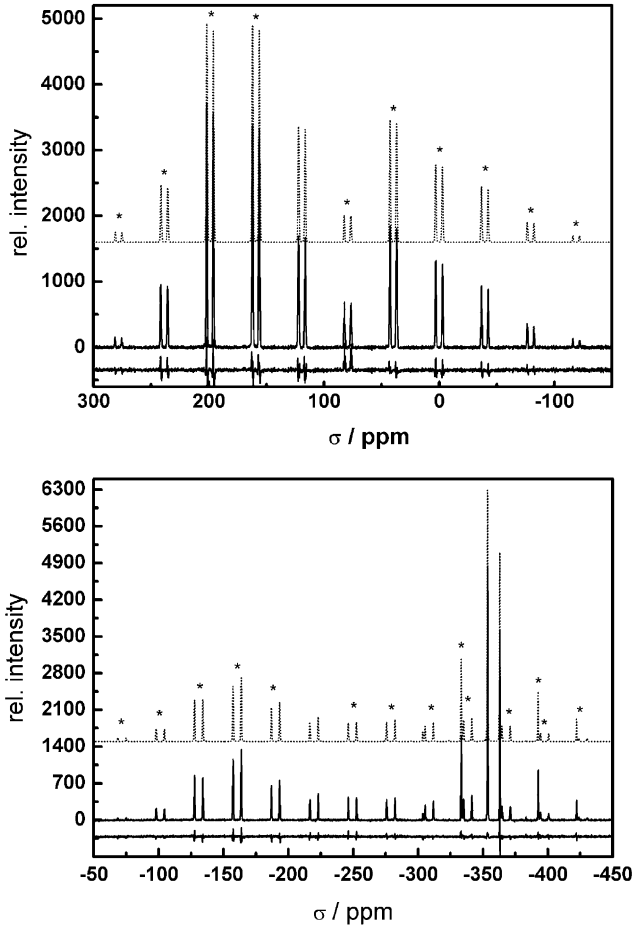

Fig. 12. Observed (solid line) and simulated (dotted line) CP-MAS-NMR spectra as well as difference plots (solid, lower line) of the nuclei ^{13}C at 5 kHz (top) and ^{15}N at 1.5 kHz spinning frequency (bottom), recorded at 305 K. For better visualization, the simulated spectra are drawn with an y-offset (arbitrarily chosen); asterisks denote spinning side bands. σ_{iso}: C1/C2: 116.4, 122.1 ppm, N1/N3: −216.8, −223.2 ppm, N2: −363.1 ppm, N4: −353.8 ppm. σ_{aniso}: C1/C2: −24872, −24932 Hz, N1/N3: −10024, −9668 Hz, N2: −3034 Hz.

4. Conclusion

In this contribution we report on the elucidation of the crystal structure of ammonium dicyanamide via temperature-dependent single-crystal X-ray and neutron powder diffraction. It can be described as a structure composed of molecular ions with alternating cation–anion contacts which are approximately equally spaced and connected by two stronger (D2⋯N3, D3⋯N1, 185–199 pm) and two weaker (D1⋯N3, D4⋯N2, 195–217 pm) hydrogen bridges. The libration corrected mean N–D bond length of the ammonium group amounts to 104 pm. The direction of the major libration axis shifts within the investigated temperature range while the pdfs of the deuterons D1 and D4 and the ammonium nitrogen exhibit increasing anisotropic character due to thermally activated librational (D) and translational (N) degrees of freedom. Evidence has been found for the commencing detachment of the deuteron D1 in the high-temperature range, serving as an initial step in the solid–solid transformation of $ND_4[N(CN)_2]$ into $D_4C_2N_4$.

The solid-state CP-MAS-NMR spectra confirm the location of all ions on general positions and of one molecule in the asymmetric unit. Thermal analyses indicate that no phase transitions occur below the onset of the solid–solid transformation of $NH_4[N(CN)_2]$ into $H_4C_2N_4$ which is in agreement with the anisotropic, yet continuous thermal behavior of the lattice constants as monitored by neutron diffraction within a temperature range between 10 and 370 K.

The frequently encountered dynamic disorder of ammonium groups due to the nature of the hydrogen potential wells is another intriguing feature of ND_4^+ mobility which can be elucidated by neutron diffraction and ^2H NMR spectroscopy. The 90° jump model of the ammonium group, consisting of 90° jumps of the deuterons around the C_2-axis of the tetrahedron and therefore requiring the nuclear density to be distributed more or less equally over eight sites, can largely be excluded on the basis of the present neutron diffraction data which allow the unambiguous identification of

exactly four sites. Other familiar jump models, however, cannot be ruled out and changes between two or more jump models within the temperature range under investigation may be possible. For the exact determination of the actual jump geometry, ^{2}H wideline NMR investigations in a broad temperature range are underway to shed light on this issue.

Acknowledgments

The authors thank Dr. H. Höppe for performing the single-crystal measurements, Dipl. Chem. S. Correll for his assistance at the powder diffraction data collection, W. Wünschheim and Dipl. Min. S. Schmid for conducting the DSC and DTA/TG measurements as well as Ch. Minke for carrying out the MAS-NMR experiments. Beam time and technical support was provided by the Mineralogical–Petrological Institute of Bonn University and the BMBF (Contract 03KLE8BN), financial support was granted from the Fonds der Chemischen Industrie (scholarship for B.V. Lotsch) and the BMBF which is gratefully acknowledged.

References

[1] A.Y. Liu, M.L. Cohen, Science 245 (1989) 841.
[2] C. Niu, Y.Z. Lu, C.M. Lieber, Science 261 (1993) 334.
[3] P.H. Fang, J. Mater. Sci. Lett. 14 (1995) 536.
[4] M.G. Down, M.J. Haley, P. Hubberstey, R.J. Pulham, A.E. Thunder, J. Chem. Soc., Dalton Trans. (1978) 1407.
[5] A.P. Purdy, E. House, C.F. George, Polyhedron 16 (1997) 3671.
[6] M. Becker, J. Nuss, M. Jansen, Z. Anorg. Allg. Chem. 626 (2000) 2505.
[7] B. Jürgens, E. Irran, J. Schneider, W. Schnick, Inorg. Chem. 39 (2000) 665.
[8] M. Becker, M. Jansen, Solid State Sci. 2 (2000) 711.
[9] E. Irran, B. Jürgens, W. Schnick, Chem. Eur. J. 7 (2001) 5372.
[10] P. Starynowicz, Acta Crystallogr. C 47 (1991) 2198.
[11] M. Becker, J. Nuss, M. Jansen, Z. Naturforsch. 55b (2000) 383.
[12] D. Britton, Y.M. Chow, Acta Crystallogr. B 33 (1977) 697.
[13] D. Britton, Acta Crystallogr. C 46 (1990) 2297.
[14] U. Berger, W. Schnick, J. Alloys Compd. 206 (1994) 179.
[15] N.-G. Vannerberg, Acta Chem. Scand. 16 (1962) 2263.
[16] B. Jürgens, E. Irran, W. Schnick, J. Solid State Chem. 157 (2001) 241.
[17] M. Becker, M. Jansen, Acta Crystallogr. C 57 (2001) 347.
[18] J.L. Manson, D.W. Lee, A.L. Rheingold, J.S. Miller, Inorg. Chem. 37 (1998) 5966.
[19] P. Jensen, S.R. Batten, G.D. Fallon, B. Moubaraki, K.S. Murray, D.J. Price, Chem. Commun. (1999) 177.
[20] B. Jürgens, H.A. Höppe, W. Schnick, Solid State Sci. 4 (2002) 821.
[21] J.L. Manson, C.R. Kmety, Q.-Z. Huang, J.W. Lynn, G.M. Bendele, S. Pagola, P.W. Stephens, L.M. Liable-Sands, A.L. Rheingold, A.J. Epstein, J.S. Miller, Chem. Mater. 10 (1998) 2552.
[22] B. Vangdal, J. Carranza, F. Lloret, M. Julve, J. Sletten, J. Chem. Soc. Dalton Trans. (2002) 566.
[23] S.R. Batten, P. Jensen, B. Moubaraki, K.S. Murray, R. Robson, Chem. Commun. (1998) 439.
[24] W. Madelung, E. Kern, Liebigs Ann. Chem. 427 (1922) 1.
[25] B. Jürgens, H.A. Höppe, E. Irran, W. Schnick, Inorg. Chem. 41 (2002) 4849.
[26] G.M. Sheldrick, SHELXS97, program for the solution of crystal structures, University of Göttingen, 1997.
[27] G.M. Sheldrick, SHELXL97, program for the refinement of crystal structures, University of Göttingen, 1997.
[28] ISIS Facility Annual Report 2001–2002, RAL-TR-2002-050.
[29] I.F. Bailey, Z. Kristallogr. 218 (2003) 84.
[30] H.M. Rietveld, J. Appl. Crystallogr. 2 (1969) 65.
[31] A.C. Larson, R.B. von Dreele, Programm GSAS General Structure Analysis System, Los Alamos National Laboratory, Los Alamos, 1994.
[32] A.E. Bennett, C.M. Rienstra, M. Auger, K.V. Lakshimi, R.G. Griffin, J. Chem. Phys. 103 (1995) 6951.
[33] M. Bak, J.T. Rasmussen, N.C. Nielsen, J. Magn. Reson. 147 (2000) 296.
[34] S.J. Cyvin, Molecular Vibrations and Mean Square Amplitudes, Elsevier Publishing Company, Amsterdam, 1968.
[35] J. Senker, H. Jacobs, M. Müller, W. Press, P. Müller, H.M. Mayer, R.M. Ibberson, J. Phys. Chem. B 102 (1998) 931.
[36] B.T.M. Willis, A.W. Pryor, Thermal Vibrations in Crystallography, Cambridge University Press, Cambridge, 1975.
[37] R.E. Dinnebier, Powder Diffraction 14 (1999) 84.
[38] C.-G. Hoelger, H.-H. Limbach, J. Phys. Chem. 98 (1994) 11803.
[39] S. Gutowsky, G.E. Pake, R. Bersohn, J. Chem. Phys. 22 (1954) 643.
[40] R. Bersohn, H.S. Gutowsky, J. Chem. Phys. 22 (1954) 653.
[41] J.W. Sprague, J.G. Grasselli, W.M. Ritchey, J. Phys. Chem. 68 (1964) 431.
[42] M. Kuhn, R. Mecke, Chem. Ber. 91 (1961) 3010.
[43] D.L. Rousseau, R.P. Baumann, S.P.S. Porto, J. Raman Spectrosc. 10 (1981) 253.
[44] K.O. Christe, W.W. Wilson, J.A. Sheehy, J.A. Boatz, Angew. Chem. Int. Ed. 38 (1999) 2004.
[45] I. Bernhardi, T. Drews, K. Seppelt, Angew. Chem. Int. Ed. 38 (1999) 2232.
[46] E.L. Wagner, D.F. Hornig, J. Chem. Phys. 18 (1950) 296.
[47] E.L. Wagner, D.F. Hornig, J. Chem. Phys. 18 (1950) 304.
[48] J. Weidlein, U. Müller, K. Dehnicke, Schwingungsspektroskopie, 2nd Edition, Georg Thieme Verlag, Stuttgart, 1988.
[49] N.B. Colthup, L.H. Daly, S.E. Wiberley, Introduction to Infrared and Raman Spectroscopy, 3rd Edition, Academic Press, London, 1990.